Optical Routers Based on Ovonic Phase Change Materials

David Strand, David V. Tsu, Robert Miller, Michael Hennessey, David Jablonski
Energy Conversion Devices, 2956 Waterview Drive, Rochester Hills, MI 48309

Abstract

The index of refraction and absorption of Ovonic Phase Change Materials based on chalcogenide alloys can differ by more than two units between the amorphous and crystalline structures. These large changes enable new types of devices such as two different switchable optical routers that we are building. One device is a phased array reflective surface. Multilayered optical stacks are designed that have a large difference in the optical phase angle of the reflected light when the included chalcogenide layer is in its amorphous or crystalline states. Since sub-wavelength mixtures of these states can also be formed, intermediate phase angle differences can also be attained. We form a linearly changing ratio of the volume fraction of the two-states across the surface of this multilayered stack to induce a non-specular and non-diffuse reflection of incident light without diffraction. The optical phase angle upon reflection off the surface of the stationary device can change by more than 180° depending on the structure of the phase change material. We have steered a 1550nm beam 2°, and we expect deflections of more than 10°. A second device is a planar photonic crystal channel add-drop multiplexer wavelength switch. The photonic crystal consists of a regular triangular array of SiO_2 -filled holes in an amorphous Ge_3Si film, sandwiched between two SiO_2 cladding layers. The pass and transfer buses consist of linear extended defects in the crystal, with the pass bus separated from each drop bus by cavity resonator defects tuned to specific wavelengths. Switching is accomplished by changing a small region of a chalcogenide alloy incorporated into each resonator between the amorphous and crystalline states. The local reconfigurability enabled by the phase change material elevates the multiplexer to an all-optical router. In both devices the steering is self latching, and sub-100 nanosecond latency enables packet-level discernment.

Introduction

One of the most remarkable properties of Ovonic phase change materials[1,2] (PCM) is the large contrast in the optical absorption and index of refraction between the crystalline and amorphous structures. This is particularly evident in the region of the near IR (NIR) spectrum that is of most interest in telecommunications region. This behavior is quite valuable in optical switching, and Ovonic phase change materials can be expected to play an important role in a range of optical switching devices. It is also worth noting that the stability of the two physical states renders the corresponding optical states completely latching. Just as electronic semiconductor devices have progressed at a rate following Moore's Law, the future of optical communication devices will likely be based on planar integration of photonic circuits. We are working to establish designs and the technology necessary to fabricate routing switches that utilize phase change material to actuate switching. In this paper we describe two such devices, a phase angle controlled stationary element (PACSE)[3] and a switchable photonic crystal.[4]

In order to realize true "broadband" telecommunication, or more accurately, widespread availability of rich content information services, switches will have to become all-optical, inexpensive and fast. These will enable a departure from the asymmetrical and hierarchical network systems of today. Instead of high capacity cores, lower capacity "edges", even lower capacity local networks, and so on out to the user, there can be high rate point-to-point transmission in a decentralized, mesh-like medium. Each point in the mesh would require essentially the capability of the core nodes of today. Ovonic phase change chalcogenides can switch in 1 – 50 nanoseconds, which is within the regime of packet or packet burst demarcation.

Information content is increasingly being transmitted on optical fibers. However, the carrying capacity of such an optical network will become limited if the network continues to rely on "OEO" switching, i.e., where incoming optical energy must first be converted into electronic energy in order for it to be electronically switched then reemitted as optical energy along the new path. Not only must the bandwidth of the electronic circuitry keep up with the extremely high bandwidth of the fiber optic cables, but as the type of content continues to expand, greater complexity will be needed to also handle the diverse formats of the data packets thereby requiring yet additional resources. For these reasons, it is generally recognized that an optical communications network will achieve its full carrying capacity by eliminating as many electronic components as possible, and replacing them with all optical component switches, or "OOO" switches. In these OOO switches, optical energy is not converted into electronic energy, but rather the optical input energy is simply redirected or steered to an optical output.

A key approach to increasing the information content on optical fibers is wavelength multiplexing. A critical part of efficient use of network resources is wavelength allocation and reallocation, so that a multiplexing/demultiplexing device coupled with fast 1x2 (drop or not) switches will become very useful. Photonic crystal channel add/drop filters[5] present a platform for performing this function in very small spaces. Localizing modes in this manner brings an important opportunity to add fast switching.

The values of n and k for the Ovonic phase change materials, $Ge_2Sb_2Te_5$ (GST-225) are shown In Figure 1. As can be seen, k for the amorphous state is low at 1550 nm, while the crystalline state is some ten times more absorptive. The refractive index n is substantially higher in the crystalline structure compared to that of the amorphous, differing by about 3 units.

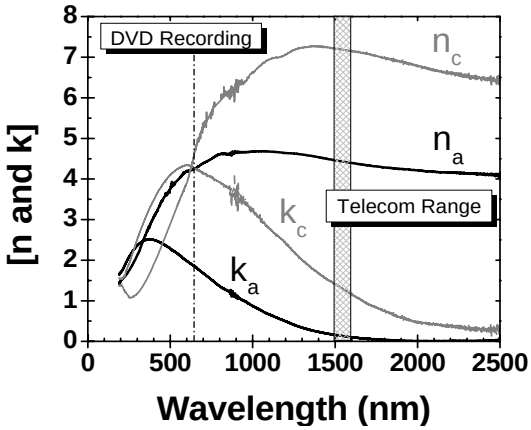

Figure 1. Optical constants [n,k] of the $Ge_2Sb_2Te_5$ PCM in its amorphous (a) and crystalline (c) states. The dashed line at 650 nm indicates the DVD optical recording wavelength, and the shaded region between 1500 and 1600 nm shows the telecom wavelengths.

Phase Angle Controlled Stationary Element

We transform the state of an Ovonic Phase Change material on the "surface" of a stationary device to achieve a phase angle taper on that surface that mimics what is produced by physical translation of the surface. We call such device a "phase angle controlled stationary element" (PACSE), to achieve non-specular (and non-diffuse) reflection.[6,7] In essence, we developed a way of applying the frequency selective surface concept,[8] that has been demonstrated for gigahertz steering,[9,10] but at the optical frequencies of telecom signals.

Figure 2 shows a schematic view of the PACSE surface for steering the telecom light beam in three different directions. The active region of the device is sub-divided into effective cells (dashed lines) on a 7 x 7 grid. The dimension of the cell is chosen to be much smaller than the wavelength of the telecom light source. Since this wavelength is nominally 1550 nm, the cell size might be 500 nm or smaller. The figure shows three different patterns of grey circular marks (top row) "recorded" in each cell of the grid. The grey circles represent regions of the multi-layer device in which its PCM layer has been changed into the amorphous state. In the regions surrounding the circles, the PCM layer remains in its crystalline state. Changing the PCM layer between its amorphous and crystalline states is achieved using energy from a focused (0.6 NA objective lens), pulsed 650 nm laser beam. In optical recording media, this type of mark diameter control leads to variations of the reflected energy that is termed "multi-level recording".[11] We have drawn the amorphous marks in Fig. 2 as the darker grey. Thus in the bottom row in Fig. 2, the grey scale represents the change in phase angle across the PACSE device, where the reflectance should be constant, i.e., like a true mirror. Since the telecom wavelength is three times larger than the cell dimension, the individual amorphous marks will not be resolved, so the phase angle will appear to be smoothly graded or tapered according to the effective media approximation when probed by the telecom NIR light. Ultimately, the steering fidelity will depend on the fidelity of multi-level mark creation. To date, we have achieved about 16 levels.

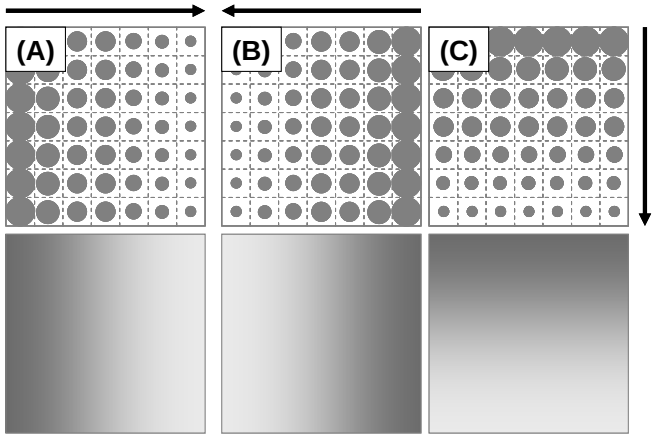

Figure 2. PACSE patterns for three different steering directions: (A) left to right; (B) right to left; and (C) top to bottom. Grey circles in the top row represent the amorphous marks in crystalline background. The bottom row represents the corresponding phase angle tapers seen by the 1550 nm light.

The optical phase angle upon reflection off this surface can change by more than 180° depending on physical state of the PCM. By manipulating the "local" phase angle in each cell in a controlled fashion across the PACSE device, we can control the reflection angle of the incident beam, i.e., we will introduce deviations of the reflection angle of the beam from the specular

direction (where angle of incidence equals the angle of reflection). In effect, the 2D cells act as an optical phased-array to steer the reflected NIR light beam. Not only can this be used to make rewritable diffractive elements, but since the "phase taper" can be made nearly continuous, the surface can also steer the beam in non-specular directions with no diffractive distortions. To date, we have steered a telecom beam 2° in one direction, and expect deflections by more than 10°. The steering is broad-banded, self latching, and potential switching speeds are expected to be less than 100 ns.

These speeds are orders of magnitude faster than the millisecond speeds achievable by physical manipulation (rotation) of the mirrors produced in micro electro mechanical systems (MEMS) devices. Although much effort has been invested in these switching devices, slow speed and high fabrication cost contribute to limit their use. Inertial effects in moving the mirror mass contribute substantially to their modest speed. The small 13 μm dimension[12] of Texas Instrument's Digital Light Processor (DLP) lead to sub-millisecond speeds. Lucent's much larger (100's of μm) Lambda Router has speed approaching 10 milli-seconds.[13] Another contributing factor of the slower Lambda Router is settling time in its variable 2-axis capability, compared to the binary-only switching state of the DLP's.

These multilayered recording devices take advantage of the very large change in the optical constants [n,k] of the PCM layer when in its amorphous versus crystalline structures. The key difference between phase change optical recording devices and PACSE devices is that the former rely principally on changes in [k] to detect the presence of binary or multi-level data. The latter relies on changes in [n] in the NIR leading to differences in the optical phase angle used to steer the beam. This is evident in the [n,k] plots[14,15] shown in Fig. 1. In fact in the optical recording case, a constant phase angle is desired to avoid interference with tracking. In the PACSE case, differences in reflectance at the telecom wavelength are not desired because this will degrade the steering performance. Maintaining a constant reflectance in the PACSE device will also ensure uniform optical transmission of the switch.

The largest angular deflection ($\Delta\theta_r$) of a light beam from the specular direction for the PACSE depends on both the change in optical phase, $\Delta\phi$, and its lateral physical dimension, where $\Delta\phi$ is the largest change in the optical phase angle obtainable by the PACSE thin film stack upon reflection. Achieving the largest deflection angle requires use of a small PACSE. It can be shown that $\Delta\theta_r$ is related to $\Delta\phi$ and the PACSE dimension according to

$$\frac{\Delta\phi}{n \times 360^{\circ}} = \sin \Delta\theta_r , \qquad (1)$$

where n is a number (≥ 1) representing the PACSE dimension in units of λ. Mirrors smaller than about twice the wavelength will introduce significant diffractive effects from the edge of the PACSE aperture. So, when $n = 2$ (where in Fig. 2, the 7 cell length extent of the grid represents 2.25 λ's), and $\Delta\phi$ is 130°, $\Delta\theta_r$ can range between ± 10.4°, representing over 20° of angular control. Device design and PCM performance will govern the extent of PACSE steering.

Figure 3 shows the results of thin film calculations[16,17] as functions of the volume fraction of crystallinity of the PCM layer. Here, we model the transformation between the amorphous and crystalline states as a continuous change, whose optical constants derive from the Bruggemann effective medium theory[18] (EMT) using the amorphous and crystalline endpoints.

In the lower part of Fig. 3, we show the "absolute" phase angle, that derives directly from the resultant complex reflectance.[17] The abrupt change at a volume fraction of about 0.1 simply means that the phase angle is cycling around 360°. No real discontinuity exists, as shown by the "relative" phase angle trace.

The optical path length change accounts for only part of the total phase angle change. Two-dimensional vector "phasor" analysis of the complex reflectance shows that changes in the Fresnel coefficients at the multi-layer interfaces can significantly enhance performance.

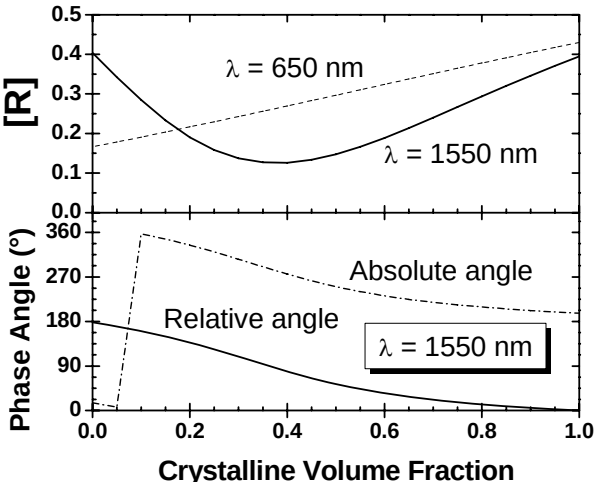

Figure 3. Calculated response of PACSE device (sample o5200) showing reflectance (top) at both 650 nm and 1550 nm wavelengths vs. volume fraction of PCM crystallinity. In the bottom panel, we show the phase angle (the absolute and relative values) for the 1550 nm illumination.

The ratio of indices between the crystalline and amorphous states of GST-225 is about 1.7 at telecom wavelengths. We have identified other $Ge_xSb_yTe_z$ compositions having ratios of 1.9. Device modeling indicates even greater phase angle differences can be achieved than what we report here. The GST-225 compound is a well studied material used in commercial optical DVD-RAM and Ovonic Universal Memory (OUM) devices. Crystalline/amorphous cycling of 10^{13} cycles have been demonstrated in OUM devices.[19]

In order to have a large change in the optical phase of the light reflected from the phase change material, we desire a large change in the index of refraction between the amorphous and crystalline states. In Fig. 4 we show the ration of the index in the crystalline state to that in the amorphous state.

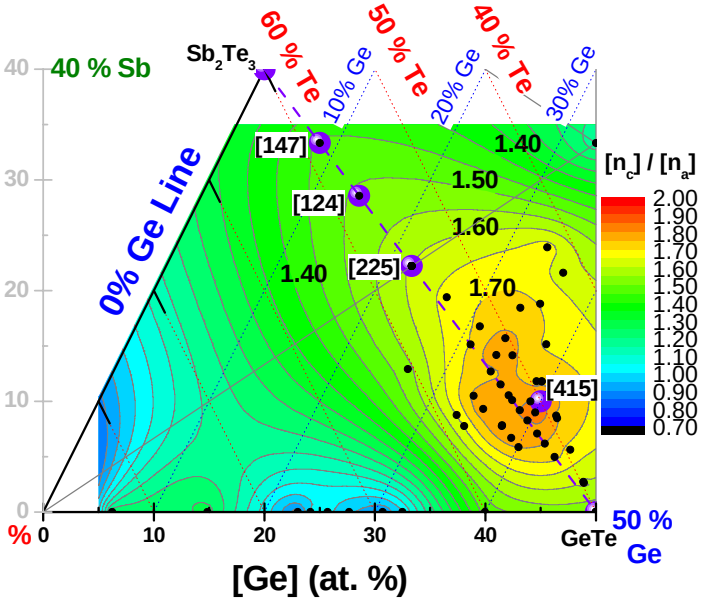

Figure 4. Quantification of the "n-ratio" at 1550 nm wavelength for the PC materials considered for the PACSE device. The black round marks are the experimental compositions, and the contours are 2-D interpolations of these points. The lowest value is found at GST-147, and it increases steadily to

Channel Drop Pc Photonic Filter

The second switching device we are building is a channel drop filter constructed from a photonic crystal, where the Ovonic PCM controls the resonance state of the switching cavity. This performs switching that is highly frequency-dependent, in the form of tunable or on/off resonators. Narrow-band channel drop resonant filters are typically passive devices[5], or devices that are switched only very infrequently. The addition of a fast, low cost switching function is extremely desirable, in that it can facilitate significant increases in network functionality downstream from the centralized core routers. Photonic bandgap (PBG) channel drop filters provide the highly touted advantage of planar optical circuits and we are designing them in a form that uses the switching properties of PCMs to important advantage.

The design we propose is based on a two-dimensional periodic slab array of holes filled with SiO_2 in a film of silicon germanium. The array is embedded between SiO_2 layers to provide mode symmetry and confinement in the vertical direction. A design for the photonic crystal is shown in Fig. 5 for purposes of illustration of the principles involved. Figure 5 shows a row of missing holes which provides an end-to-end mode-guiding defect in the crystal. This structure is the input bus. At one or more locations along the input bus, defect rows parallel and locally identical to it, called drop buses, are presented spaced some number of periods away. In the crystal region between the buses in each such location, a resonator structure comprised primarily of an enlarged hole is inserted. Additional holes in the vicinity of the resonator are altered in size to tune the structure so that odd and even modes are balanced, providing the optimal mode transfer.

When the enlarged holes are located in such a manner that they and the two buses considered together possess local mirror plane symmetry in directions both perpendicular and parallel to the buses, the local system acts as a complete channel drop for the input wavelength that corresponds to the resonance of the cavity. This means that all of the power at that wavelength leaves the input bus

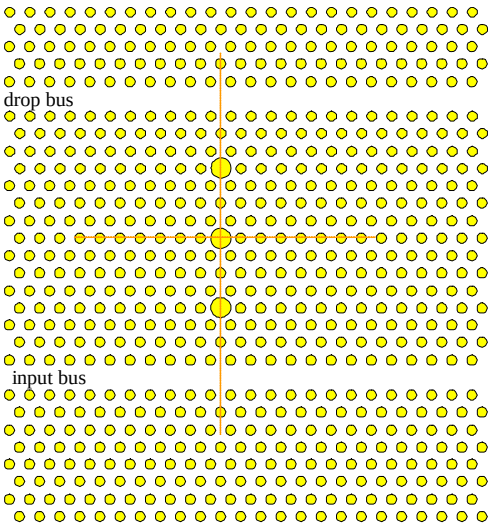

Figure 5. Cascade of three dipole-like resonant cavities between input bus and drop bus showing two mirror symmetry planes.

and transfers to the drop bus. The cavity resonant frequency is a function of the enlarged hole diameter and the shape and size of its neighbors. Dropping additional frequency bands is accomplished by additional distinct cavity structures down-stream from the first. The presence of a second identically enlarged hole at a channel drop along with a concomitant increase in the spacing between the buses helps provide a flat-topped, steep side-walled response function to pass the entire channel spectral width without increased crosstalk, in much the same way as cascaded filters in electronics.[20]

It is generally necessary that the intrinsic decay rate of the cavity (due to absorption and radiation) be much lower than the extrinsic decay rate (due to the buses), in order to perform complete transfer. It has also been shown[21] that if the intrinsic decay rate somehow becomes much greater than the extrinsic decay rate in the same design, not only does the transfer fail to occur, but no mode can couple to the cavity at all, so that all of the energy remains in the input bus, except for any small overlap of the bus' evanescent "tail". When the phase change material is in the amorphous phase, the intrinsic decay rate is small, and when in the crystalline state the decay rate is very high, as the absorption of the crystalline material makes the structure lossy. Each of the enlarged cavity holes is partly comprised of an Ovonic phase change alloy. Each cavity hole, therefore, becomes switchable by changing the phase between a lossy state and a relatively non-lossy state. Switching is accomplished by changing the structure of the chalcogenide between amorphous and crystalline, using a short wavelength diode laser.

It is important that there exists high contrast in permittivity between the host (SiO_2) and surrounding medium in the photonic crystal device. We use an alloy of silicon and germanium that has a very low absorption in the NIR, and which has an index of refraction of 3.94. The photonic crystal device has better performance when the optical properties of the Ovonic material closely match those of the high index material (SiGe alloy) in the photonic crystal matrix. We use an Ovonic chalcogenide alloy to switch the resonator between its lossy and non-lossy states. For the non-lossy state, the PCM must have absorption lower than GST-225. To achieve this we alloyed small amounts of additional elements into GST-225. Figure 6 shows the change in the optical properties we accomplished by this modification. We were able to lower k down below 0.01. This result is shown in Fig. 6.

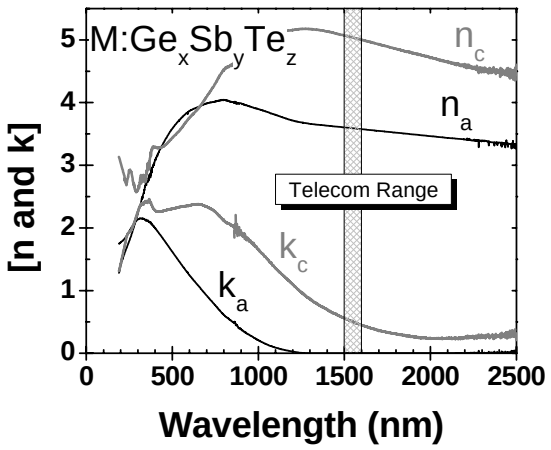

Figure 6. [n,k] for M:$Ge_xSb_yTe_z$ in amorphous (a) and crystalline (c) states

We use a planar topology comprised of a two-dimensional lattice in a three-dimensional slab. This format cannot have a complete band gap, but rather only a gap in the lattice plane.[22] Planar topology is immensely superior in terms of cost. It inherits all of the economy of planar processing, including wafer scale processing, size scaling, availability of highly evolved toolsets and accumulated experience. Further, we are making a switchable device, and although Ovonic phase change materials can be switched electrically or optically, a photonic crystal would be profoundly perturbed by the presence of electrical conductors, so optical actuation is preferred. This requires line-of-sight access for a laser beam which the 2D slab design provides.

Although most early theoretical work in two-dimensional photonic crystals used a square array of high-index dielectric columns ("rods") through a lower index continuum as the preferred platform, providing a simple model that could exhibit a large bandgap, we have found the opposite arrangement (array of low index dielectric columns ("holes") in a high index continuum) to be preferable in terms of leading to a more manufacturable device. Our modeling shows that the optimum slab thickness of a square array for the materials we are using is about 800 nm (1.8 times the lattice period), with a high index rod diameter of about 200 nm. For the low-index-hole slab, the corresponding values are both a thickness and hole diameter of about 225 nm (about 0.6 times the period), an almost eightfold reduction in aspect ratio. In view of the challenges in fabrication at this scale, this reduction in aspect ratio is decisive.

To achieve an index contrast with SiO_2 that is sufficient to give us a large enough band gap to cover a large portion of the telecom bands, a dielectric with an index greater than that of silicon (n ~ 3.4) is required for the slab. Pure crystalline germanium has an index of about 4.3, but its absorption edge is too close to the 1550 nm telecom wavelength to have the low absorption required to propagate practical distances. Alloys of silicon and germanium up to 75% germanium are transparent at 1550 nm.[23] This composition results in an index very close to 4.0, which

allows a band gap of about 80 nm at 1550 nm, enough to span the C and L bands, and easily covering each band separately.

Photonic Band Gap Modeling

Numerical computation pertaining to the photonic crystal has been performed using a parallel cluster of networked computers. Frequency domain analysis was done using an adapted version of the MIT code available online, while FDTD analysis used code largely rewritten by Jeffrey Reed (Science Applications International Corporation (SAIC)).

Band structure for various infinite (pure 2D) hole crystal slabs were first found, from which parameters to optimize the center of the band gap at 1550 nm and to maximize the width were derived. The optimal dimensions to maximize the gap width are found for the SiO_2 / $SiGe_3$ system to be a 225 nm slab thickness, with 225 nm diameter holes in a regular triangular periodic array whose period is 375 nm.

Next defect structures were introduced, first for waveguides. The result for a "missing row of holes" waveguide, in Figure 7, shows that the waveguide supports two modes, but with two frequency intervals that are each single moded. When the light cone for the slab is taken into account, only the mode in the lower frequency part of this gap appears useful, since most of the upper mode is in the radiating regime. For point defects which are to comprise resonant cavities, it is simplest to start with those supporting monopole modes, which are obtained most directly by enlarging the diameter of a hole, and for which a hole size is free to vary over a wide range of resonant frequencies without exciting a higher-order mode.

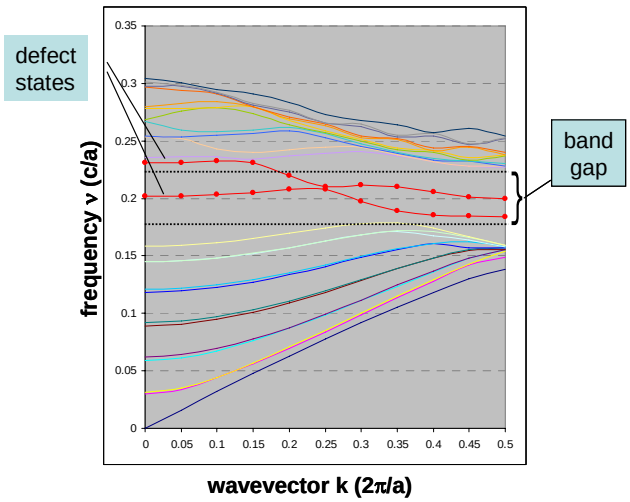

Figure 7. Dispersion plot of missing-row line defect in a triangular hole slab. There are two modes in the gap, but two intervals that are single-moded.

Theoretical considerations show that channel dropping using monopole modes is only possible if there is at least one pair of identical monopoles present, which support two degenerate modes, one symmetrical and one anti-symmetrical with respect to the vertical plane between them, and are also symmetric with respect to a mirror plane through the two cavities.[24,25] For the design we use, the symmetry planes are shown in Fig. 8. In the presence of the bus and drop waveguides, part of the symmetry of the system is lost, and the odd mode and even mode acquire slightly different frequencies and decay bandwidths; thus other types of symmetry have to be introduced to restore degeneracy.

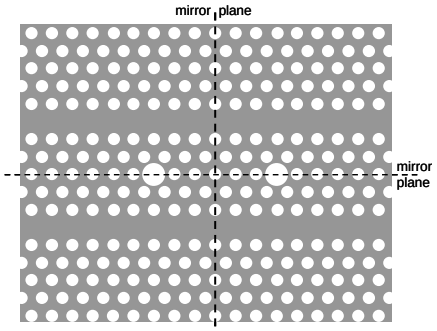

Figure 8. Dual monopole cavities and waveguides, showing the two required symmetry planes.

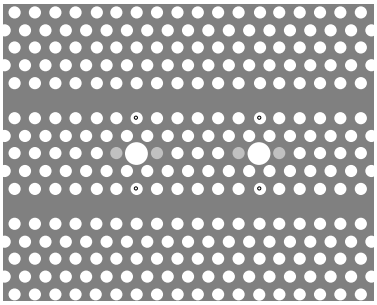

Figure 9. Dual monopole cavities with possible balancing holes indicated by dots or shading; we alter the shaded holes.

To make the decay widths identical, there is a phase relationship required relating wave vector amplitude in the bus, and number of periods between the holes, which has only a few discrete solutions.[24] Thus the resonant frequency

used must match that of the waveguide mode at one of the values of wave vector allowed for a given spacing. This means that the spacing should be chosen carefully, so that the operating point is one where the waveguide mode is in a good place: not near a band edge or a multimoded condition, and with adequate group velocity. For our materials, this is best achieved for a spacing of six periods.

Once the waveguides are present, a pair of cavities interact by two different processes, one direct and one via the waveguides. To make the center frequencies equal, it is necessary to make these two processes offset each other. We do this by slight adjustment of diameters of some holes that lie directly in one or the other decay path, but doing so with enough such holes so as not to change the overall symmetry of the structure. It turns out that for the spacings chosen, these are very nearly balanced already, so only a slight change in neighboring holes to the cavities (Fig. 9) is needed to bring the center frequencies together.

We are also considering several other (standing wave) structures, including single cavities that support degenerate states (which for the unperturbed C_{6v}-symmetric lattice are limited to dipoles and quadrupoles), dual hexapole cavities, locally disordered lattice cavities, and traveling wave resonators such as rings and disks.

Conclusion

We have shown that Ovonic PCMs can be used as the active component layer of a flat surfaced multi-layered optical device which can change the phase angle of the reflected beam by substantial amounts (about 180°). The PACSE device makes use of refractive index ratio's of more than 1.7 times in the PCM layer. We have shown that a smooth taper of the phase angle can be created on this flat surface and a NIR telecom beam can be steered without distortion. We have demonstrated 2° steering, and we expect more than 10° steering. The PACSE device is a 1 x N optical broad band switch

We introduced a strategy for a application of Ovonic phase change materials to build high speed photonic wavelength switches. We have established that photonic bandgap structure is an appropriate platform on which to build them, and present a design to do so. We have optimized the ternary chalcogenide GST-225 to perform the absorptive/transparent function in a switchable channel add/drop filter.

Acknowledgements

This work was inspired and supported by Stan Ovshinsky, whose guidance and leadership are invaluable, and a grant from the Advanced Technology Program, National Institute of Standards in Technology, under the U.S. Department of Commerce, contract number 70NANB3H3066.

References

1. S.R. Ovshinsky and H. Fritzsche, "Reversible Structural Transformations in Amorphous Semiconductors for Memory and Logic," Metall. Trans. **2**, 641 (1971).
2. J. Feinleib, J. de Neufville, S.C. Moss, and S.R. Ovshinsky, "Rapid Reversible Light-Induced Crystallization of Amorphous Semiconductors," Appl. Phys. Lett. **18**, 254 (1971).
3 D.V. Tsu, R.O. Miller and D. Strand, "All optical broadband steering by Phase Angel Controlled Stationary Element (PACSE) mirrors," SPIE, Photonics West 2006, *Proceedings of SPIE* Vol. **6123**, Session 7, WG Engineering II, 24 January 2006 [6123-34]
4 R.O. Miller, D.V. Tsu, J.A. Reed and D. Strand, "Photonic crystal nanosecond wavelength switches," SPIE, Photonics West 2006, Proceedings of SPIE Vol. **6124**, Optoelectronic Integrated Circuits X, Session 3 - Micro/Nano-Scale OEICs, 23 January 2006, [6124-11].
5. B.E. Little, S.T. Chu, H.a. Haus, J. Foresi, and J.P. Laine, J. Lightwave Technol. **15**, 998 (1997).
6. David Tsu, "Phase angle controlled stationary elements for wavefront engineering of electromagnetic radiation", US Patent No. 6768666, July 27, 2004.
7. David Tsu, "Phase angle controlled stationary elements for long wavelength electromagnetic radiation", US Patent No. 6882460, April 19, 2005.
8. R. Ulrich, "Far-infrared properties of metallic mesh and its complementary structure", Infrared Physics **7**, p37-55 (1967).
9. W.W. Lam, C.F. Jou, H.Z. Chen, K.S. Stolt, N.C. Luhmann, Jr., and D.B. Rutledge, "Millimeter-Wave Diode Grid Phase Shifters ", IEE Trans. On Microwave Theory and Techniques **36**, 902-907 (1988).
10. L.B. Sjogren, H.X.Liu, X. Qin, C.W. Domier, and N.C. Luhmann, Jr., "Phased array operation of a diode grid impedance surface", IEE Trans. On Microwave Theory and Techniques **42**, 565-572 (1994).
11. M.P. O'Neill, T.L. Wong, in *Optical Data Storage 2000*, Whistler, B.C., Conference Digest (May 2000).

12. L.J. Hornbeck, "Deformable-Mirror Spatial Light Modulators," in *Spatial Light Modulators and Applications III*, SPIE Critical Reviews, Vol. **1150**, 86-102 (1989).
13. "Lucent Introduces Optical Router," Presstime Bulletin, in Photonics Spectra **34**, 18 (Jan. 2000); "Lucent Terminates the LambdaRouter," Article in LightReading.com (Aug. 15, 2002).
14. David V. Tsu, "Obtaining optical constants of thin $Ge_xSb_yTe_z$ films from measurements of reflection and transmission", J. Vac. Sci. Technol. A **17**, 1854-1860 (1999).
15. ECD's *OptiCon* software numerically solves for [n,k] and film thickness from [R,T] measurements.
16. ECD's *EMA* software provides multilayer thin film optical calculations where each layer's optical properties can depend on two endpoint materials, that can be combined according to effective medium theory (e.g., Maxwell-Garnet, Bruggemann, etc.).
17. O.S. Heavens, "*Optical properties of thin solid films"* (Dover, New York, 1991), Chapter 4
18. D.E. Aspnes, "Optical properties of thin films," Thin Solid Films **89**, 249 (1982).
19. S.R. Ovshinsky, "Amorphous and Disordered Materials – The Basis of New Industries", in *Bulk Metallic Glasses*, edited by William L. Johnson, Akihisa Inoue and C.T. Liu, Mat. Res. Soc. Symp. Proc. **554**, 399 (1999).
20. J. Fu, S. He, S. Xiao, "Analysis of channel-dropping tunneling processes in photonic crystals with multiple vertical multimode cavities," J. Phys. A **33** (43) 7761 (2000).
21. S. Fan, P.R. Villeneuve, J.D. Joannopoulos and H.A. Haus, "Loss-induced on/off switching in a channel add/drop filter," PRB **64** (24), Art. 245302, 2001.
22. S.G. Johnson, et al., "Linear waveguides in photonic crystal slabs," Phys. Rev. B **62** 8212-22 (2000).
23. E.D. Palik, *Handbook of Optical Constants*, London: Academic Press (1985).
24. S. Fan, P.R. Villeneuve, et al., PRB 59 (24) "Theoretical analysis of channel drop tunneling processes," pg. 15882 (1999).
25. C. Manolatou, M.J. Khan, et al., "Coupling of modes analysis of resonant channel add-drop filters," IEEE Journal of Quant Electronics, **35** (9) 1322 (1999).